

Spectral assessment of soil properties in semi-arid tropical regions of southern Karnataka Plateau

M. Lalitha, S. Dharumarajan, C. Gomez, Rajendra Hegde, Arti Koyal, Shivanand Khandal, BN. Shashikumar & S. Parvathy

To cite this article: M. Lalitha, S. Dharumarajan, C. Gomez, Rajendra Hegde, Arti Koyal, Shivanand Khandal, BN. Shashikumar & S. Parvathy (2022): Spectral assessment of soil properties in semi-arid tropical regions of southern Karnataka Plateau, Archives of Agronomy and Soil Science, DOI: [10.1080/03650340.2022.2134565](https://doi.org/10.1080/03650340.2022.2134565)

To link to this article: <https://doi.org/10.1080/03650340.2022.2134565>



Published online: 24 Oct 2022.



Submit your article to this journal



Article views: 21



View related articles



View Crossmark data



RESEARCH ARTICLE



Spectral assessment of soil properties in semi-arid tropical regions of southern Karnataka Plateau

M. Lalitha^a, S. Dharumaranjan^a, C. Gomez^{b,c}, Rajendra Hegde^a, Arti Koyal^a, Shivanand Khandal^a, BN. Shashikumar^a and S. Parvathy^a

^aICAR-National Bureau of Soil Survey and Land Use Planning, Regional Centre, Bangalore, India; ^bIndo-French Cell for Water Sciences, IRD, Indian Institute of Science, Bangalore, India; ^cIRD, INRAE, Institut Agro, LISAH, Univ. Montpellier, Montpellier, India

ABSTRACT

The present study assessed the visible and short wave infrared (VNIR-SWIR) laboratory spectroscopy coupled random forest regression (RF) technique for predicting soil properties in the southern Karnataka Plateau, India. The spectral data acquired for about 228 profile samples were used to predict key soil properties. The RF model fits well for the spectral prediction of clay ($R^2 = 0.65$), sand ($R^2 = 0.60$), cation exchange capacity ($R^2 = 0.74$), field capacity ($R^2 = 0.65$) and permanent wilting point ($R^2 = 0.72$). Wherein soil organic carbon was poorly predicted with an R^2 of 0.22 and RPD of 1.2 due to its lower content and narrow range (0.8 to 20 g kg⁻¹). The spectral assessment by PCA showed that the first (50%) and third (34%) components had high spectral variation and significantly correlated with soil properties such as pH, CEC, clay, FC, and PWP related to wavelengths indicating clay minerals and iron oxides. However, the second component had less spectral variation (13%) that is related to wavelengths indicating various organic components and correlated well with SOC. Thus, the VNIR-SWIR spectroscopy could be a suitable supplementary method for rapidly predicting soil properties related to clay minerals and iron oxides.

ARTICLE HISTORY

Received 5 April 2022
Accepted 5 October 2022

KEYWORDS

Soil survey; laboratory VNIR-SWIR spectroscopy; soil properties; random forest regression; semiarid tropical

Introduction

Soil is a natural resource that delivers ecosystem services to humans through the realization of a series of soil processes (Dominati et al. 2010). Soil exhibits a large pedodiversity at all scales (Tennesen 2014) and recognized as a critical resource for most global environmental sustainability challenges (McBratney et al. 2014). The pedodiversity supports various biogeochemical processes that result in a particular soil type, which can show considerable variations in its performance (Bouma et al. 2012). Therefore, assessing soil functional properties in real-time and scale requires advanced techniques to quantify the soil properties more rapidly for making management decisions (Hewitt et al. 2015). For example, the geo-referenced soil information system (SIS) requires implementing a series of complex, expensive, and time-consuming soil analyses. Soil reflectance spectroscopy is a fast and inexpensive analytical method that predicts soil properties by relating it with spectral data in the VNIR-SWIR (400–2500 nm) spectral regions. These spectral regions are widely used in soil assessments because of high absorption features due to stretching and bending of

covalent bonds leading to direct absorption or overtones of absorption features (Demattê and da Silva Terra 2014).

The distinctive spectral signature of each soil property and its correlation with spectra is the principle behind its prediction (first-order predictions) (Terra et al. 2015; Naimi et al. 2022). The efficiency of VNIR-SWIR spectra to predict numerous physical, chemical, and biological properties of soils using multivariate regression models has been well demonstrated (Rossel et al. 2006b; Cécillon et al. 2009; Asgari et al. 2020a). For example, the physical properties such as clay, sand, Field Capacity (FC), and Permanent Wilting Point (PWP) (Mouazen et al. 2005; Lagacherie et al. 2008; Gomez and Coulouma 2018); chemical properties such as pH, Cation Exchange Capacity (CEC) (Pirie et al. 2005; Stenberg et al. 2010), carbonates (Asgari et al. 2020b); biological parameters such as biomass C and N (Reeves et al. 2006; Chodak et al. 2007), and nutrient properties such as Soil Organic Carbon (SOC), P, N, K, Ca, Na, Mg, and Fe (Udelhoven et al. 2003; Mouazen et al. 2007; Gomez et al. 2008; Rodionov et al. 2015) were well predicted by researchers across the globe with a range of prediction accuracy. The mineralogical compositions such as kaolinite, gibbsite, hematite, goethite, illite, and oxides and hydroxides of Fe and Al, etc., were predicted by Clark et al. (1990), Brown et al. (2006), and Rossel et al. (2006b).

The soil properties will be linked with soil spectral data through various models such as PLSR (Partial Least Square Regression) (Cozzolino and Moron 2003), PCR (Principal Component Regression) (Islam et al. 2003), SMLR (Stepwise Multiple Linear Regression) (Bartholomeus et al. 2012). The random forest model is the machine-learning algorithm accounting for the statistical approximation of both linear and non-linear relationships of co-variants (Breiman 2001; Zeraatpisheh et al. 2017). The QRF (quantile regression forest) model is a new random forest model that has the advantage of building the prediction interval (PI) by analyzing the distribution of observed response variables at each tree leaf (Meinshausen 2006). The models for a particular prediction have been selected based on the data kind, the relationship between spectral data and dependent variables, and the data transformation method. Accordingly, each model performs differently for a given region.

Ben-Dor et al. (2002) highlighted that spectral prediction is significantly related to 1) co-variations between spectral data and soil variable (first-order prediction), 2) co-variation between soil variables (first-order predictors X other soil properties), and 3) variation (range) within each observed soil variable. However, the variation between soil property and co-variation within each soil property depends on pedological processes influenced by biophysical and environmental variables, which will vary according to the influence of dominant soil forming factors in tropical, subtropical, and temperate regions. Gomez and Coulouma (2018) emphasized that a prediction model built at a regional scale performed poorly when it was validated at the local scale and the need for model development at the local scale for better prediction. The development of regional-specific soil spectral libraries is, therefore, a priority for soil research worldwide (Brown et al. 2006).

Several successful VNIR spectral models have been developed to predict soil properties of agronomic importance in India (Dwivedi et al. 1981; Singh et al. 2014). For example, the soil properties linked to nutrient management in precision farming (Vibhute et al. 2018); assessment of soil salinity properties (Srivastava et al. 2017); assessment of functional soil properties (Saxena et al. 2003; Srivastava et al. 2004; Kadupitiya et al. 2010; Solanke et al. 2021); hydraulic property prediction (Santra et al. 2009; Dharumarajan et al. 2022); soil moisture assessment (Gulfo et al. 2012); aggregate size segregation (Sarahjith et al. 2014); soil microbiological properties (Mondal et al. 2017) have been assessed spectroscopically using different models.

The predictive ability of soil VNIR-SWIR spectroscopy for estimation of multiple soil properties at the national to the regional scale largely depends on the quality of the calibration set, which must be representative of the physiographic landforms, diversity of soils, and land use type (Cécillon et al. 2009; Pinheiro et al. 2017). Since the calibration data set's quality differs based on pedodiversity, local calibrations for each agro-ecoregions are obligatory. These highlights the requirement for more prominent spectral libraries representative of India's pedodiversity to predict the properties of Indian soils at the national and regional levels (Das et al. 2015). In this context, the present study was aimed

with the objective 1) to assess the VNIR-SWIR spectra for the prediction of selected soil properties using the RF model and 2) to interpret the prediction variation of soil properties of the southern Karnataka plateau.

Materials and methods

Study area

Southern Karnataka plateau, also known as the Mysore Plateau, is an undulating terrain characterized by hills, hill ranges, rolling lands, interfluves, and valleys with an elevation ranging from 600 to 900 m above mean sea level (AMSL). The isolated residual hills in the ranges reach the height of 1500–1750 m AMSL. The isolated hills are steeply sloping, dominated by boulders and rocks with little soil cover. The major soils were shallow to very deep, somewhat excessively to well-drained, red gravelly loam to gravelly clay, and red clay soils (red ferruginous soils). They were classified as Ustropelts, Kandiustalfs, Paleustalfs, Rhodustalfs, and Haplustalfs (in ustic areas) (Shivaprasad et al. 1998). Granite gneiss, schist, and quartzite are the primary geological substrates. The region receives a mean annual rainfall of 450–925 mm. The study region was divided into four agro-climatic zones based on the length of growing period (LGP), such as 150 to 180, 120 to 150, 90 to 120, and < 90 days. Rainfed farming is generally practiced. The principal crops grown are finger millet, maize, groundnut, sorghum, and pulses. The detailed flowchart depicting the steps involved in soil properties prediction is given in Figure 1.

Soil database

The soil profile samples collected under the SUJALA III project (Hegde et al. 2018) were utilized for the present study. The soil profiles were dug either to 2 m or up to the parent material, whichever is earlier in the identified location, based on landform, slope, and land use. Soil layers of different depths were identified based on morphological characteristics of the profile (colour, texture, structure, etc.), and soil samples were collected from each horizon of the representative soil profiles (Soil Survey Staff 2010). The soil depth varied from very shallow (< 25 cm) to very deep (> 150 cm). A total of 228 geo-referenced horizon-wise samples were collected from 46 profiles for laboratory analysis. The samples were adequately labelled, air-dried, pounded, and sieved through a 2-mm sieve. The 2-mm sieved samples were used to analyze soil pH and electrical conductivity (EC) in a 1:2.5 soil water ratio (Jackson et al. 1973). The soil organic carbon was analyzed in 0.2-mm sieved samples as per Walkley and Black's (1934) method. Soil particle-size analysis was carried out by the international pipette method (Piper 1966). Soil cation exchange capacity (CEC) was estimated by the 1 N ammonium acetate (pH-7) method (Schollenberger and Simon 1945). Water retention characteristics of the soil at –33 kPa [field capacity (FC)] and –1500 kPa [permanent wilting point (PWP)] were determined gravimetrically using pressure plate apparatus (Richard 1954).

Acquisition of VNIR-SWIR soil spectra

The soil spectra were acquired from 350 to 2500 nm reflective domain in 2-mm sieved samples using the ASD (Analytical Spectral Devices Inc., USA) Spectroradiometer. The soil samples were thoroughly mixed and placed in a petri dish with 15 cm diameter and 2 cm height that was focused by four halogen light sources (40 W). The samples were uniformly levelled in the dish to avoid heap causing measurement error. Before sample measurement, it was calibrated with the white reflectance plate. The sensor captured the reflectance, and each measurement was the mean of 30 internal scan replications made by the instrument. Each sample was measured thrice, and middle spectra were used for the property prediction. White reference was acquired before and after for each sample set of five. The spectral resolution was 3 nm for 350 to 1000 nm spectral ranges and 10 nm for 1000 to

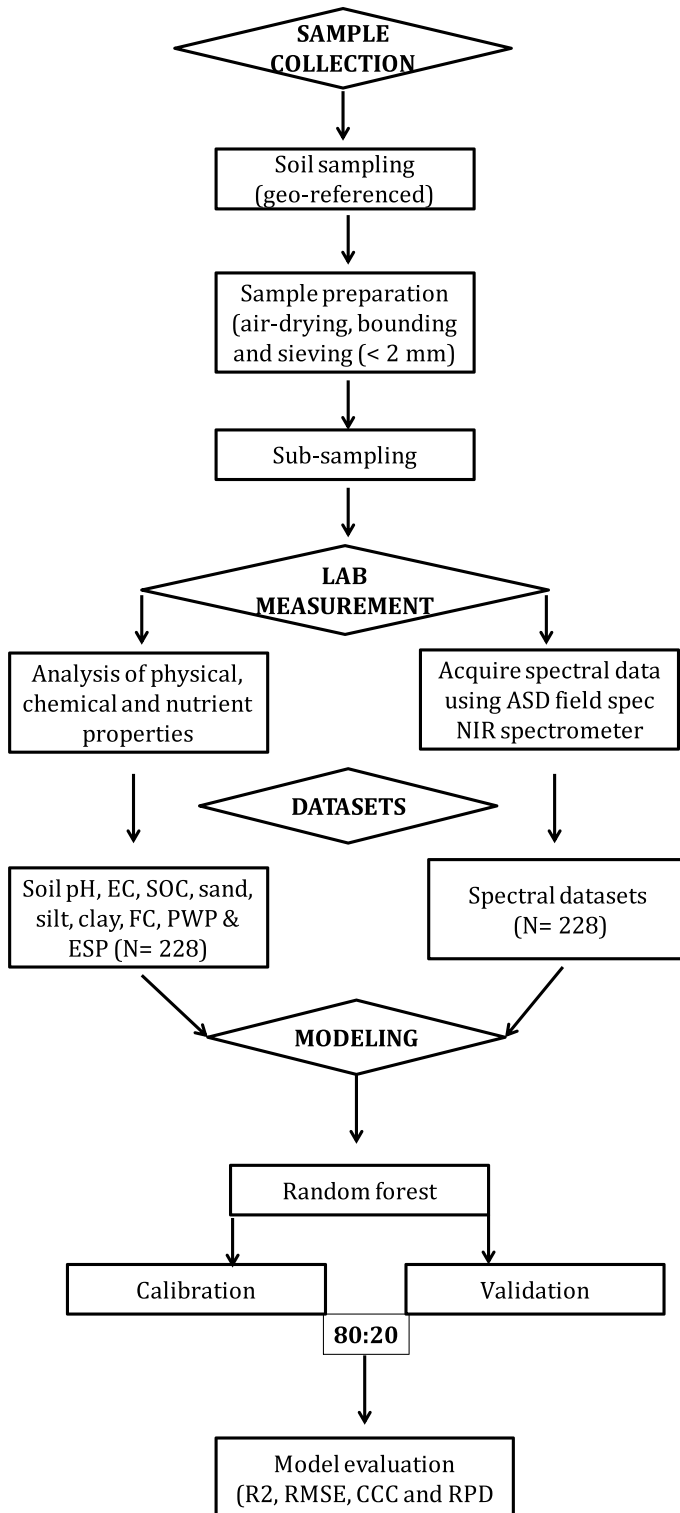


Figure 1. Flowchart depicting soil property prediction from VNIR-SWIR spectral data.

2500 nm spectral range. A total of 2151 spectral bands acquired by ASD software were used to predict soil properties (www.asdi.com).

Prediction model and evaluation

The Random Forest (RF) model was used to predict the soil properties from spectral data (Breiman 2001). The RF algorithms need minimal data pre-processing, and the data can be used without transformation (Kuhn and Johnson 2013), and it handles both linear and non-linear relationships of the data. Moreover, the RF model works based on two levels of randomization at each tree in the forest (Breiman 2001). RandomForest 4.6 package in R was used for prediction. The ntree of 1000 and mtry of 7 were used in the model. The ratio of 80:20 was adopted for training and testing. The model performance was evaluated using R^2 , RMSE, CCC, and RPD of testing datasets with 100 iterations.

$$\text{Root Mean Square Error (RMSE)} = \sqrt{\sum_{i=1}^N \frac{(\hat{y}_i - y_i)^2}{N}}$$

$$\text{Bias} = \sum_{i=1}^N \frac{y_i}{N} - \sum_{i=1}^N \frac{\hat{y}_i}{N}$$

$$\text{Concordance Correlation Coefficient (CCC)} = \frac{2\rho\sigma_{y_i}\sigma_{\hat{y}_i}}{\sigma_{y_i}^2 + \sigma_{\hat{y}_i}^2 + (\mu_{y_i} - \mu_{\hat{y}_i})^2}$$

$$\text{Ratio of performance to deviation (RPD)} = \frac{SD}{RMSE}$$

where N is the number of samples, y_i is the measured property value of i^{th} soil sample, \hat{y}_i is the predicted property value of i^{th} soil sample, and \bar{y} is the mean of the observed value. μ_{y_i} and $\mu_{\hat{y}_i}$ are the means of observed and predicted values and σ_{y_i} , $\sigma_{\hat{y}_i}$ are the corresponding variance and ρ is the Pearson correlation coefficient. SD is the standard deviation of observed values. As per Terra et al. (2015), the R^2 value was interpreted as 1) the model well fitted to predict the property accurately ($R^2 > 0.75$); 2) fairly predicted ($R^2:0.50-0.75$); 3) unreliable ($R^2 < 0.50$) model. The threshold value used for interpretations of RPD were RPD > 2.5 for excellent predictions; $2.5 > \text{RPD} > 2.0$ for very good predictions; $2.0 > \text{RPD} > 1.8$ for good predictions (Rossel et al. 2006a).

Results and discussions

Statistics of soil properties

The soil reaction varied from strongly acidic to strongly alkaline (pH: 4.5 to 9.1), and soils were non-saline (mean: 0.1 dS m⁻¹). Soil organic carbon content was very low, ranging from 0.8 to 20 g kg⁻¹, reflecting irregular distribution with depth. The SOC in surface soil ranged from 2.4 g kg⁻¹ to 20 g kg⁻¹. The variation may be attributed to the cumulative effect of crop residue addition and loss due to various crop management practices (Lalitha and Kumar 2016). The SOC in the subsurface soils ranged from 0.5 g kg⁻¹ to 8.1 g kg⁻¹, and as low as 0.8 g kg⁻¹ were found in bottom layers (>150 cm depth) because of negligible residue addition. The mean and standard deviations of soil particle size distributions showed that sand ($53.5\% \pm 16.5$) was the predominant fraction, followed by clay ($31.5\% \pm 13.1$) and silt ($15.0\% \pm 6.4$). The soil particle size contents are mainly influenced by parent material and erosion rate (Lalitha et al. 2021a). The field capacity and permanent wilting point ranged from 4.1–70.9% and 2.1–41.0%, respectively. The cation exchange capacity of the soils varied from 1.2 to 52.6 cmol (+) kg⁻¹ (Table 1). The cation and water retention characteristics of the soils are mainly controlled by the amount and kind of clay minerals present in the soil (Lalitha et al. 2019). The skewness coefficient for soil properties ranged from –0.8 to 4.2, and except for soil pH and sand,

Table 1. Summary statistics of soil properties.

Properties	pH	EC (dS m ⁻¹)	OC	Sand	Silt	Clay	FC	PWP	CEC (cmol (+) kg ⁻¹)
					(%)				
Mean	7.6	0.10	0.40	53.5	15.0	31.5	22.2	11.4	14.7
Min	4.5	0.02	0.08	4.4	2.0	5.8	4.1	2.1	1.2
Max	9.1	0.48	2.00	92.3	36.0	67.8	70.9	41.0	52.6
SD	0.9	0.08	0.23	16.5	6.4	13.1	9.5	6.3	9.5
Kurtosis	0.1	2.98	10.49	0.7	0.7	-0.2	5.4	3.1	2.9
Skewness	-0.8	1.57	2.22	-0.6	1.0	0.3	1.8	1.5	1.6

other properties were positively skewed. The skewness and kurtosis coefficients for clay were 0.3 and -0.2, showing a fairly symmetrical distribution. The properties such as EC, OC, FC, PWP, and CEC were highly skewed, reflecting asymmetric distribution. The variation might be due to the differential pedogenic process operating over different horizons of soil profiles (up to 2 m or till to the hard substratum), controlling the biogeochemical cycle, and intern influencing the vertical distribution of soil physical and chemical properties. A very high coefficient value for kurtosis was observed for EC, OC, FC, PWP, and CEC, possibly because of outliers (Brys et al. 2004).

Spearman correlations between soil properties

Correlation analysis helps to identify the prediction approximation of individual soil properties based on the correlation between the properties of first-order predictions (SOC, sand, clay, and Fe and Al oxides) (Terra et al. 2015) and other soil properties. The Spearman correlations among soil properties showed that soil pH had a significant positive correlation with soil properties except for SOC (-0.29, p < 0.01) and sand fractions (-0.31, p < 0.01). The same trend was observed for EC, which had a significant negative correlation with sand fractions (-0.22, p < 0.01). Interestingly, the SOC that could be detected directly by spectroradiometer called the first-order prediction (reported from humid and temperate regions) was not significantly correlated with other soil properties (Table 2). In humid or temperate soils, the non-spectrally detectable properties were well predicted through second-order predictions due to a strong correlation between soil properties and SOC.

Table 2. Spearman correlation between soil properties and first three PCA scores of the spectra (N = 228).

Soil properties	pH	EC	SOC	Sand	Silt	Clay	CEC	FC	D1	D2	D3
pH									-0.51**	0.26**	-0.31**
EC	0.58**								-0.70**	0.14*	-0.14*
SOC	-0.29**	0.22**							-0.27**	-0.22**	0.18**
Sand	-0.31**	-0.22**	0.07						0.18**	-0.18**	0.69**
Silt	0.43**	0.34**	0.03	-0.43**					-0.32**	0.41**	-0.07
Clay	0.37**	0.16*	-0.06	-0.81**	0.28**				-0.01	0.06	-0.80**
CEC	0.67**	0.59**	0.04	-0.61**	0.49**	0.68**			-0.57**	0.12	-0.54**
FC	0.58**	0.29**	-0.14*	-0.77**	0.55**	0.83**	0.76**		-0.22**	0.29**	-0.66
PWP	0.50**	0.30**	-0.07	-0.78**	0.42**	0.89**	0.76**	0.89**	-0.24	0.15*	-0.79**

*. Correlation is significant at the 0.05 level (2-tailed)

**. Correlation is significant at the 0.01 level (2-tailed)

The soil particle size fractions, CEC, and water retention parameters were significantly correlated ($p < 0.05$) among each other. Particularly sand fraction had a significant ($p < 0.05$) negative correlation, while the silt and clay fractions had a significant positive correlation ($p < 0.05$) with all the soil properties. Among that clay was strongly correlated with field capacity (0.83, $p < 0.01$) and permanent wilting point (0.89, $p < 0.01$). It indicates that the surface charges on the clay particles or clay mineralogy make up the soil cation and water retention characteristics.

Description of VNIR-SWIR spectra related to soil order properties

The major soil order identified in the southern Karnataka plateau was Alfisols (red ferruginous soil), followed by Inceptisols. The soil spectral reflectance measured for different horizons of major soil order profiles is given in Figure 2. The spectral signatures exhibited by the soil orders were almost similar in curve shape across the wavelength region, particularly the highest absorbance features at 1900, followed by 2200 and 1400 nm. The Inceptisol order showed a similar reflectance pattern

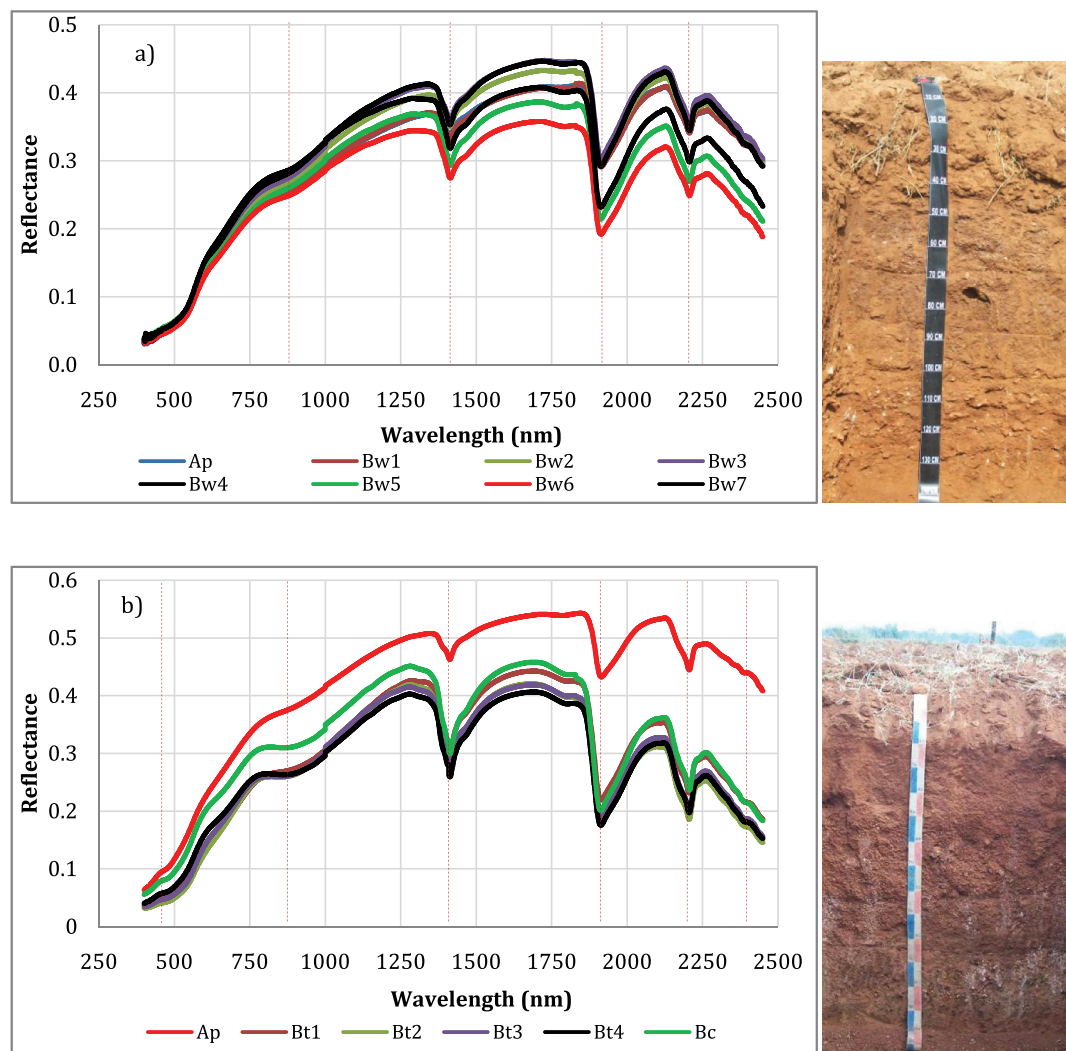


Figure 2. Spectral reflectance curve of soils from different horizons of a) Inceptisols and b) Alfisols.

across the soil layers (Bw1-Bw7) whereas, in Alfisols, the surface horizon had a high reflectance feature compared to subsurface horizons of the profile might be due to the high sand content of the surface. It is the peculiar characteristic of Alfisols (having an argillic diagnostic horizon featured by the accumulation of illuvial clay from the surface horizon (Bt1-Bt4)) (Soil Survey Staff 2010).

The absorption feature at 850 nm was more prominent in Alfisols, and mainly, the subsurface had a sharp absorption curve compared to surface soils. The presence of iron and aluminium minerals in the illuviated clay minerals of subsurface layers might have been the cause for a more prominent reflectance curve at 850 nm (Richter et al. 2009). The absorption feature for OH stretching ranged from 1410 to 1415 nm; H-O-H absorption features were observed from 1910 to 1920 nm, and Al-OH stretching from 2200 to 2210 nm for different layers. The absorbance feature for OH stretching was in the reflectance range of 0.270 to 0.365 for different horizons of Inceptisol. Wherein the Alfisols, the range was between 0.255 and 0.305, which might be related to the presence of 1:1 or 2:1 clay minerals.

Similarly, the spectral feature for H-O-H and Al-OH stretching was in the reflectance range of 0.190 to 0.235 and 0.245 to 0.365 for Inceptisols. In the case of Alfisols, the reflectance range was 0.175 to 0.225 and 0.185 to 0.210 for H-O-H and Al-OH groups, and it might be related to the presence of residual water or hydroxides of Fe and Al, respectively. The absorption features related to the compounds of soil organic matter observed at 2390 to 2400 nm (Stevens et al. 2008; Vasques et al. 2009) were not prominent for both Alfisols and Inceptisols. Overall, comparing the spectral reflectance of the two soil orders, the absorbance pattern and spectral curve shape were more prominent in Alfisols than Inceptisols might be because of comparatively more Fe-bearing minerals in the soil.

Predictions of soil properties

Soil cation exchange capacity was predicted better with an accuracy of R^2 : 0.74, and RPD of 1.9, followed by permanent wilting point (R^2 : 0.72, RPD: 1.9). Soil field capacity (R^2 : 0.65, RPD: 1.6), clay (R^2 : 0.65, RPD: 1.7), sand (R^2 : 0.60, RPD: 1.6) (Table 3) were moderately well predicted. The soil silt had a low R^2 value of 0.22. The CCC for ESP was negligible; low for SOC; moderate for pH, EC, and silt; high

Table 3. Prediction performance of RF models in predicting various soil quality properties.

Properties	R^2	CCC	RMSE	BIAS	RPD
pH	0.53 (0.14)	0.65 (0.11)	0.60 (0.10)	-0.02 (1.49)	1.5
EC	0.48 (0.21)	0.64 (0.11)	0.06 (0.01)	0.00 (0.01)	1.3
SOC	0.22 (0.23)	0.40 (0.20)	0.19 (0.07)	0.01 (0.03)	1.2
Sand	0.60 (0.1)	0.72 (0.07)	10.33 (1.52)	0.04 (1.49)	1.6
Silt	0.46 (0.17)	0.59 (0.13)	4.47 (0.91)	0.11 (0.80)	1.4
Clay	0.65 (0.05)	0.76 (0.03)	7.64 (0.51)	0.08 (1.05)	1.7
CEC	0.74 (0.07)	0.82 (0.04)	4.88 (0.85)	-0.07 (0.62)	1.9
FC	0.65 (0.08)	0.76 (0.05)	5.80 (1.02)	-0.17 (0.77)	1.6
PWP	0.72 (0.05)	0.81 (0.04)	3.28 (0.43)	-0.14 (0.43)	1.9

CCC- Concurrent correlation coefficient

Values in parenthesis are SD

for sand, clay, CEC, FC, and PWP (Hinkle et al. 2003). Soil organic carbon was poorly predicted with an R^2 of 0.22, and RPD of 1.2 against an average R^2 of 0.81 in the NIR region and R^2 of 0.78 in the visible region reported by Rossel et al. (2006a) (Figure 3). The good prediction could be due to the wide range of SOC content in the humid regions (Bellon-Maurel and McBratney 2011; Terra et al. 2015). Unlike humid tropical areas, where the SOC content ranged from 0.1 to 106 g kg⁻¹ (Pinheiro et al. 2017), the SOC observed in the study area was very narrow (0.008 to 2 g kg⁻¹) due to the higher decomposition rate aided by high temperature and cultivation practices (Lalitha et al. 2021b). The EC, SOC, and silt were poorly predicted (1.4 > RPD > 1.0), whereas sand, clay, and FC were fairly predicted (1.8 > RPD > 1.4) and good predictions were observed for CEC and PWP (2.0 > RPD > 1.8) (Rossel et al. 2006a). Overall, it indicates that the spectral prediction of the random forest model was good for soil properties that had a wide range (clay, sand, CEC, FC, and PWP) in contrast to those varying in a narrow range (pH, EC, and SOC).

Most important variable

The most important variable based on the Gini score deployed by the model in predicting various soil properties is given in Figure 4. The most important variable (IncNodePurity) of SOC, pH, EC, and silt did not show any peak trend in the spectral region due to poor model performance. In the case of sand, the Gini score was high, around 400, 1900, and 2000 nm spectral range with peaks at 409, 410, 411, 1897, 1900, 1930, 1985, 1987, 2002, and 2072 nm. The Gini score for clay was in the spectral range of 2200, 2300, and 2500 nm, with peaks of more than 125 at 2210, 2435, and 2442 nm, respectively. The peak at 2210 nm might be related to OH-Al, and OH modes as in montmorillonite, kaolinite, and illite (Gomez and Coulouma 2018), and the peak around 2400 nm range might be related to muscovite or biotite (Post and Noble 1993). The Gini score for CEC was high in the spectral range of 1914 to 2098 nm, with peaks at 1914, 1936, and 2099 nm. The soil water-retention characteristics, such as field capacity and permanent wilting point, resemble the Gini score of soil CEC. The highest peaks were observed for FC and PWP at 1995, 2039, 2118, 2251, and 2299 nm and 1919, 1948, 2028, 2041, and 2248 nm, respectively. It reflects that soil mineral composition and clay mineralogy plays a direct role in soil CEC and water retention characteristics of these soils. Thus, the peak around the 1900 nm region might be related to the high specific surface area of 2:1 clay minerals, which could firmly adsorb water molecules on their surface (Stenberg 2010). Similarly, the peak around 2200 nm regions might be related to interlayer lattice water present in the clay minerals as hydrated cations, which may increase with increasing clay content (Bishop et al. 1994; Marakkala Manage et al. 2018).

VNIR-SWIR spectra and soil properties

The spectral variations related to the reflectance behaviour of different soils were analyzed through principal component analysis (PCA) (Figure 5). The first three components showed a cumulative variation of 97% after varimax rotation, and their eigenvectors were used for assessing the reflectance behaviour across the VNIR-SWIR region. The PC1, which explained 50% of the spectral variation, has significant deep troughs at 1413 and 1916 nm that are related to overtones of O-H and H-O-H stretch vibrations, indicating the presence of water bound in the interlayer clay lattice (Bishop et al. 1994). Wherein the troughs at 2206, 2356, and 2384 nm are associated with varying Al content and the isomorphous substitution of Fe and Mg for Al in the inorganic soil components (Ben-Dor et al. 1999; Ng et al. 2019). Overall, the PC1 group may indicate the presence of expanding clay minerals such as montmorillonite, vermiculite, and illite group minerals that are most dominant in the soils of Inceptisols soil order (Rossel and Behrens 2010). The reflectance of these minerals varies according to their swelling capacity, hydration property, and occurrence of interlayer cations (Stevens et al. 2013). This assignment is supported by the significant correlation between PC1 score and soil properties related to clay mineralogy (second-order variable) such as CEC

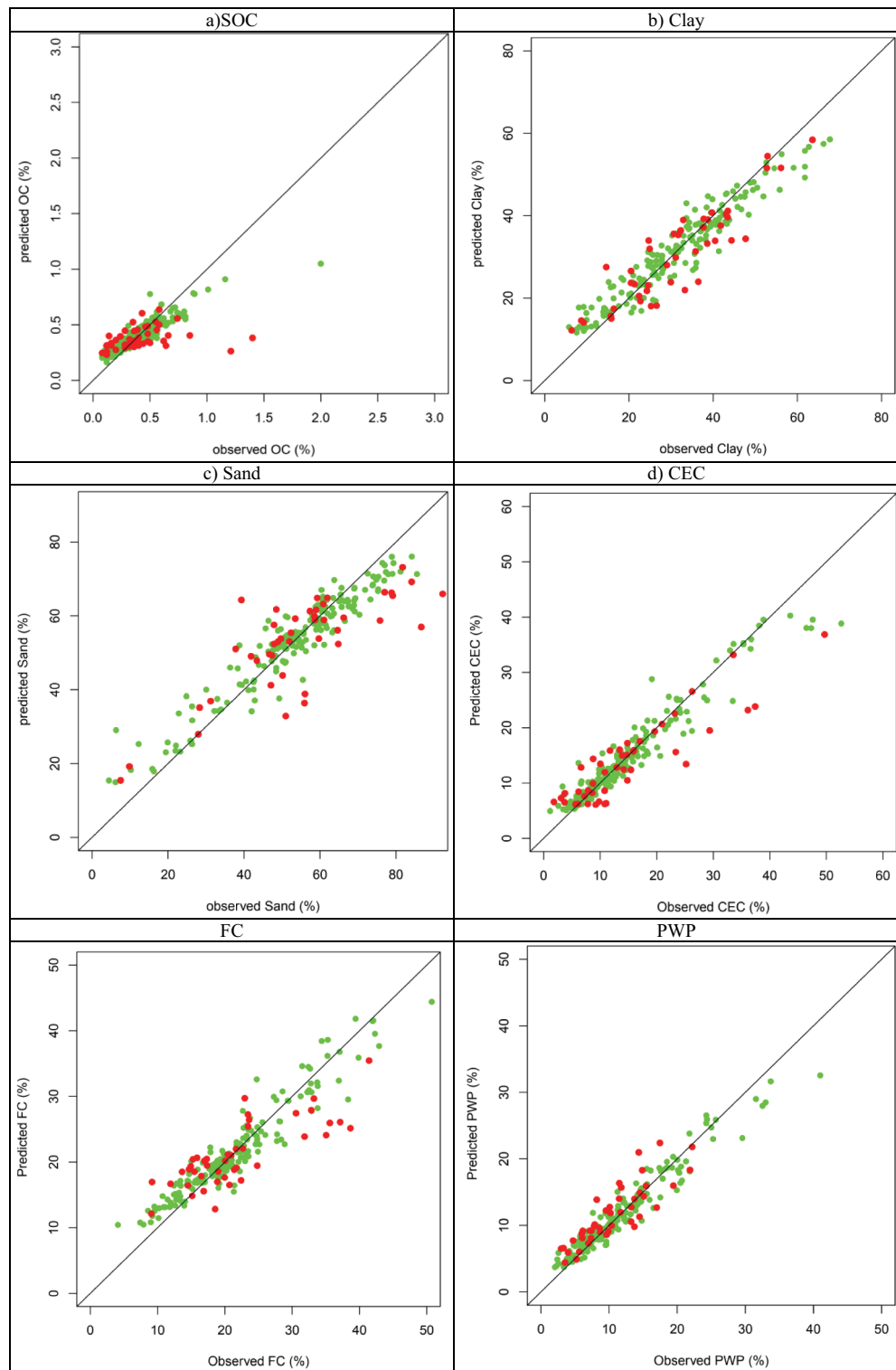


Figure 3. Scatter plots of predicted and observed soil properties of southern Karnataka plateau using RF model (green points-calibration data, red points-validation data).

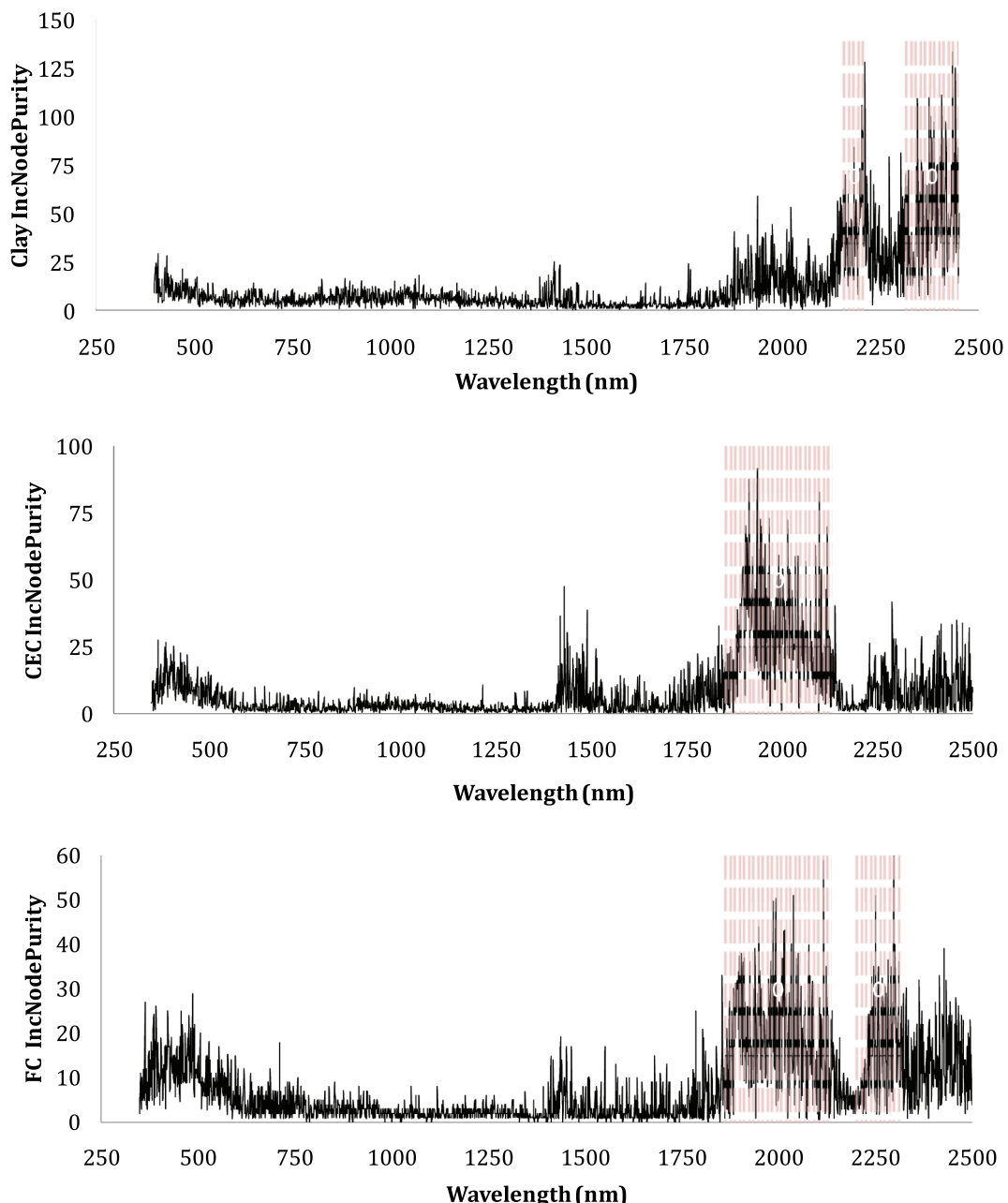


Figure 4. Most important variable score from the random forest model for soil properties in the southern Karnataka plateau.

(-0.570 , $p < 0.01$), silt (-0.318 , $p < 0.01$), FC (-0.215 , $p < 0.01$), and PWP (-0.239 , $p < 0.01$). The PC2 explained only 13% of the spectral variation due to the low amount of organic components available for spectral interaction. The eigenvector undulation from 500 to 900 nm might be due to the absorption deviation of different soil organic components in the visible region. The slight and important features which are difficult to distinguish at 1436, 1895, and 2290 nm are related to COO-, COOH, and CO-NH₂ bonds present in different organic components such as protein, humic acids, fulvic acids, starch, lignin, etc. (Ben-Dor et al. 2002), and the adsorbed water on the organic

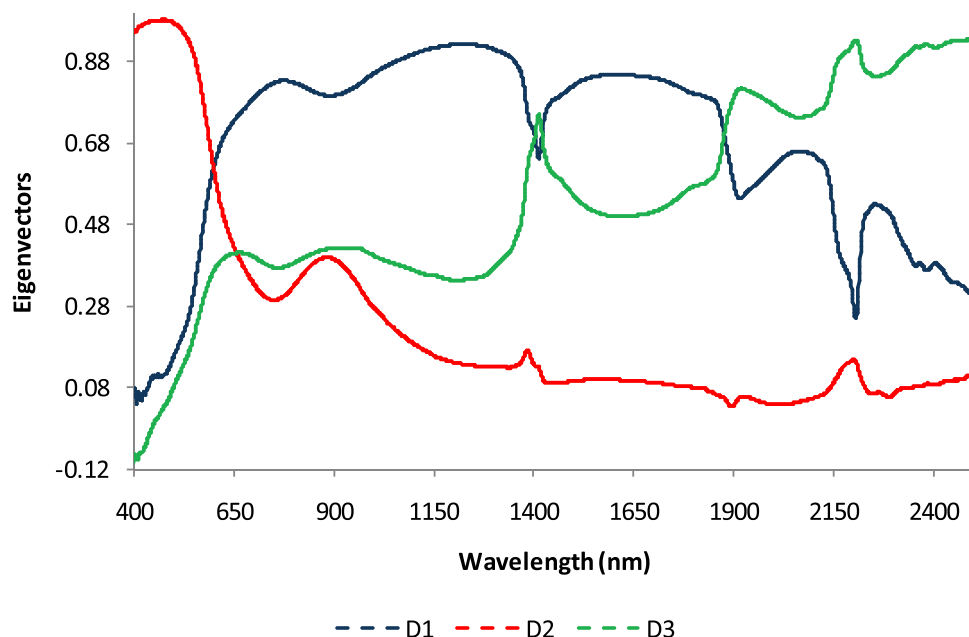


Figure 5. Eigenvectors of the first three PCA scores.

matter. The significant peaks at 881, 1384, and 2201 nm might be related to chelation with metal cations. These are explained by the significant negative correlation between PC2 score and SOC (-0.177 , $p < 0.01$) and a weak correlation with other soil properties. The eigenvector of the third PC showed a spectral variation of 34%, and it has well-defined peaks at 661, 945, 1413, 1920, and 2206 nm, which are related to the presence of iron oxides. The presence of hematite (Fe_2O_3) and goethite (FeOOH) in Alfisols (red ferruginous soils) might be the reason for the peaks at 661 and 945 nm (Rossel and Behrens 2010). The peaks in other regions might be due to microcrystalline kaolinites with structured Fe formed through metamorphic alteration of plagioclase feldspar and biotite micas during the paleoclimatic history of humid tropics, which remain as remnant clay minerals in soils of prevailing semi-arid tropics (Pal 2021). The third PC scores were strongly correlated with pH (-0.309 , $p < 0.01$), EC (-0.140 , $p < 0.01$), clay (-0.803 , $p < 0.01$), CEC (-0.539 , $p < 0.01$), PWP (-0.663 , $p < 0.01$) and FC (-0.787 , $p < 0.01$) indicating the significance of iron oxide minerals of red ferruginous soil.

Conclusion

Assessment and prediction of soil properties of southern Karnataka plateau by VNIR-SWIR spectrometry coupled with Random Forest algorithm showed that the prediction performance was low for SOC, moderate for pH, EC, and high for sand, clay, CEC, FC, and PWP. The spectral interpretation with the help of the PCA score revealed that soil properties such as CEC, silt, FC, and PWP were in one group concerning wavelength absorption by clay minerals. The second group focused on the wavelength absorption region related to SOC content, and the low prediction for soil organic carbon is due to its low content and narrow range in the soils. The third group consists of pH, EC, clay, CEC, PWP, and FC, which are related to the wavelength absorption region by iron oxides. The good prediction observed for sand, clay, CEC, FC, and PWP suggests that clay mineralogy is the prime factor that controls the functional capacity of inherent soil properties. The good performance of sand, clay, CEC, FC, and PWP suggests that VNIR-SWIR spectrometry coupled with the Random Forest

algorithm could be an efficient supplement tool enabling rapid assessments of inherent soil properties for resource management. Developing a robust spectral library incorporating both spectral and soil data acquired and analyzed by adopting quality control standards may further advance and innovate solutions for rapid characterization of soil resources

Acknowledgements

The authors thank Karnataka Watershed Development Department and World Bank for funding the SUJALA III project. Authors acknowledge ATCHA, ANR-16-CE03-0006 project for supporting the work.

Disclosure statement

No potential conflict of interest was reported by the author(s).

References

- Asgari N, Ayoubi S, Dematté JAM, Dotto AC. [2020b](#). Carbonates and organic matter in soils characterized by reflected energy from 350–25000 nm wavelength. *J Mt Sci.* 17(7):1636–1651. doi:[10.1007/s11629-019-5789-9](https://doi.org/10.1007/s11629-019-5789-9).
- Asgari N, Ayoubi S, Jafari A, Dematté JAM. [2020a](#). Incorporating environmental variables, remote and proximal sensing data for digital soil mapping of USDA soil great groups. *Int J Remote Sens.* 41(19):7624–7648. doi:[10.1080/01431161.2020.1763506](https://doi.org/10.1080/01431161.2020.1763506).
- Bartholomeus H, Schaepman-Strub G, Blok D, Sofronov R, Udaltssov S. [2012](#). Spectral estimation of soil properties in siberian tundra soils and relations with plant species composition. *Appl Environ Soil Sci.* 241535:1–13. doi:[10.1155/2012/241535](https://doi.org/10.1155/2012/241535)
- Bellon-Maurel V, McBratney A. [2011](#). Near-infrared (NIR) and mid-infrared (MIR) spectroscopic techniques for assessing the amount of carbon stock in soils – critical review and research perspectives. *Soil Biol Biochem.* 43(7):1398–1410. doi:[10.1016/j.soilbio.2011.02.019](https://doi.org/10.1016/j.soilbio.2011.02.019).
- Ben-Dor E, Irons JR, Epema GF. [1999](#). Soil reflectance. In: Rencz A, Ryerson R, editors. *Remote sensing for the earth sciences, Manual of remote sensing*. 3rd ed. New York, NY: John Wiley & Sons.
- Ben-Dor E, Patkin K, Banin A, Karnieli A. [2002](#). Mapping of several soil properties using DAIS-7915 hyperspectral scanner data - a case study over clayey soils in Israel. *International Journal of Remote Sensing.* 23(6):1043–1062. doi:[10.1080/01431160010006962](https://doi.org/10.1080/01431160010006962).
- Bishop JL, Pieters CM, Edwards JO. [1994](#). Infrared spectroscopic analyses on the nature of water in montmorillonite. *Clays Clay Miner.* 42(6):702–716. doi:[10.1346/CCMN.1994.0420606](https://doi.org/10.1346/CCMN.1994.0420606).
- Bouma J, Stoorvogel JJ, Sonneveld MPW. [2012](#). Land evaluation for landscape units. In: Huang PM, Li Y, Sumner ME, editors. *Handbook of soil sciences: properties and processes*. 2nd ed. CRC Press/Taylor Francis; 34(1–20).
- Breiman L. [2001](#). Random forests. *Machine Learning.* 45(1):5–32. doi:[10.1023/A:1010933404324](https://doi.org/10.1023/A:1010933404324).
- Brown DJ, Shepherd KD, Walsh MG, Mays MD, Reinsch TG. [2006](#). Global soil characterization with VNIR diffuse reflectance spectroscopy. *Geoderma.* 132(3–4):273–290. doi:[10.1016/j.geoderma.2005.04.025](https://doi.org/10.1016/j.geoderma.2005.04.025).
- Brys G, Hubert M, Struyf A. [2004](#). A robust measure of skewness. *J Comput Graph Stat.* 13(4):996–1017. doi:[10.1198/106186004X12632](https://doi.org/10.1198/106186004X12632).
- Cécillon L, Barthès BG, Gomez C, Ertlen D, Génot V, Hedde M, Stevens A, Brun JJ. [2009](#). Assessment and monitoring of soil quality using near-infrared reflectance spectroscopy (NIRS). *Eur J Soil Sci.* 60:5:770–784. doi:[10.1111/j.1365-2389.2009.01178.x](https://doi.org/10.1111/j.1365-2389.2009.01178.x).
- Chodak M, Niklińska M, Beese F. [2007](#). Near-infrared spectroscopy for analysis of chemical and microbiological properties of forest soil organic horizons in a heavy-metal-polluted area. *Biol Fertil Soils.* 44(1):171–180. doi:[10.1007/s00374-007-0192-z](https://doi.org/10.1007/s00374-007-0192-z).
- Clark RN, King TVV, Klejwa M, Swayze GA, Vergo N. [1990](#). High spectral resolution reflectance spectroscopy of minerals. *J Geophys Res Solid Earth.* 95(B8):12653–12680. doi:[10.1029/JB095iB08p12653](https://doi.org/10.1029/JB095iB08p12653).
- Cozzolino D, Moron A. [2003](#). The potential of near-infrared reflectance spectroscopy to analyse soil chemical and physical characteristics. *J Agric Sci Technol.* 140(1):65–71. doi:[10.1017/S0021859602002836](https://doi.org/10.1017/S0021859602002836).
- Das BS, Sarathjith MC, Santra P, Sahoo RN, Srivastava R, Routray A, Ray SS. [2015](#). Hyperspectral remote sensing: opportunities, status and challenges for rapid soil assessment in India. *Curr Sci.* 860–868. doi:[10.18520/CS/V108/15/860-868](https://doi.org/10.18520/CS/V108/15/860-868)
- Dematté JAM, da Silva Terra F. [2014](#). Spectral pedology: a new perspective on evaluation of soils along pedogenetic alterations. *Geoderma.* 217:190–200. doi:[10.1016/j.geoderma.2013.11.012](https://doi.org/10.1016/j.geoderma.2013.11.012)

- Dharumarajan S, Lalitha M, Gomez C, Vasundhara R, Kalaiselvi B, Rajendra Hegde. 2022. Prediction of soil hydraulic properties using VIS-NIR spectral data in semi-arid region of Northern Karnataka Plateau. *Geoderma Reg.* 28:e00475. <https://doi.org/10.1016/j.geodrs.2021.e00475>.
- Dominati E, Patterson M, Mackay A. 2010. A framework for classifying and quantifying the natural capital and ecosystem services of soils. *Ecol Econ.* 69(9):1858–1868. doi:[10.1016/j.ecolecon.2010.05.002](https://doi.org/10.1016/j.ecolecon.2010.05.002).
- Dwivedi RS, Singh AN, Raju KK. 1981. Spectral reflectance of some typical Indian soils as affected by tillage and cover types. *J Indian Soc Remote Sens.* 9(2):33–40. doi:[10.1007/BF02991462](https://doi.org/10.1007/BF02991462).
- Gomez C, Coulouma G. 2018. Importance of the spatial extent for using soil properties estimated by laboratory VNIR/SWIR spectroscopy: examples of the clay and calcium carbonate content. *Geoderma.* 330:244–253. doi:[10.1016/j.geoderma.2018.06.006](https://doi.org/10.1016/j.geoderma.2018.06.006).
- Gomez C, Lagacherie P, Coulouma G. 2008. Continuum removal versus PLSR method for clay and calcium carbonate content estimation from laboratory and airborne hyperspectral measurements. *Geoderma.* 148(2):141–148. doi:[10.1016/j.geoderma.2008.09.016](https://doi.org/10.1016/j.geoderma.2008.09.016).
- Gulfo E, Sahoo RN, Sharma RK, Khanna M. 2012. Soil moisture assessment using hyperspectral remote sensing. Proceedings of the Second National Workshop on Challenges and Opportunities of Water Resources Management; November 2012; Tana Basin, Upper Blue Nile Basin, Ethiopia. Blue Nile Water Institute: Bahir Dar University.
- Hegde R, Niranjana KV, Srinivas S, Danorkar BA, Singh SK. 2018. Site-specific land resource inventory for scientific planning of Sujala watersheds in Karnataka. *Curr Sci.* 115(4):645–652. doi:[10.18520/cs/v115/i4/644-652](https://doi.org/10.18520/cs/v115/i4/644-652).
- Hewitt A, Dominati E, Webb T, Cuthill T. 2015. Geoderma Soil natural capital quantification by the stock adequacy method. *Geoderma.* 241–242:107–114. doi:[10.1016/j.geoderma.2014.11.014](https://doi.org/10.1016/j.geoderma.2014.11.014)
- Hinkle DE, Wiersma W, Jurs SG. 2003. Applied statistics for the behavioral sciences. Boston; London: Houghton Mifflin; p. 1–663.
- Islam K, Singh B, McBratney A. 2003. Simultaneous estimation of several soil properties by ultra-violet, visible, and near-infrared reflectance spectroscopy. *Soil Res.* 41:1101–1114. doi:[10.1071/SR02137](https://doi.org/10.1071/SR02137)
- Jackson ML, Miller RH, Forklin RE. 1973. Soil chemical analysis. New Delhi: Prentic-Hall of India Pvt. Ltd.
- Kadupitiya HK, Sahoo RN, Ray SS, Chakraborty D, Ahmed N. 2010. Quantitative assessment of soil chemical properties using visible (VIS) and near-infrared (NIR) proximal hyperspectral data. *Trop Agric.* 158:41–60.
- Kuhn M, Johnson K. 2013. Applied predictive modeling. New York; NY: Springer; p. 1–600. doi:[10.1007/978-1-4614-6849-3](https://doi.org/10.1007/978-1-4614-6849-3)
- Lagacherie P, Baret F, Feret J-B, Netto JM, Robbez-Masson JM. 2008. Estimation of soil clay and calcium carbonate using laboratory, field and airborne hyperspectral measurements. *Remote Sens Environ.* 112(3):825–835. doi:[10.1016/j.rse.2007.06.014](https://doi.org/10.1016/j.rse.2007.06.014).
- Lalitha M, Dharumarajan S, Kumar KS, Parvathy S, Koyal A, Kalaiselvi B, Hegde R, Singh SK. 2019. Evaluation of soil moisture retention characteristics using pedo-transfer functions for soils of dry semi-arid region. *J Soil Water Conserv India.* 47(2):163–171.
- Lalitha M, Hegde R, Dharumarajan S, Koyal A. 2021b. Soil fertility evaluation in rainfed regions of different agro-climatic zones of Karnataka, India. *Agric Res.* 11:215–218. doi:[10.1007/s40003-021-00561-z](https://doi.org/10.1007/s40003-021-00561-z)
- Lalitha M, Kumar P. 2016. Soil carbon fractions influenced by temperature sensitivity and land use management. *Agrofor Syst.* 90(6):961–964. doi:[10.1007/s10457-015-9876-9](https://doi.org/10.1007/s10457-015-9876-9).
- Lalitha M, Kumar KSA, Nair KM, Dharumarajan S, Koyal A, Khandal S, Kaliraj S, Hegde R. 2021a. Evaluating pedogenesis and soil Atterberg limits for inducing landslides in the Western Ghats, Idukki District of Kerala, South India. *Nat Hazards.* 106(1):487–507. doi:[10.1007/s11069-020-04472-0](https://doi.org/10.1007/s11069-020-04472-0).
- Marakkala Manage LP, Greve MH, Knadel M, Moldrup P, De Jonge LW, Katuwal S. 2018. Visible-near-infrared spectroscopy prediction of soil characteristics as affected by soil-water content. *Soil Sci Soc Am J.* 82(6):1333–1346. doi:[10.2136/sssaj2018.01.0052](https://doi.org/10.2136/sssaj2018.01.0052).
- McBratney A, Field DJ, Koch A. 2014. The dimensions of soil security. *Geoderma.* 213:203–213. doi:[10.1016/j.geoderma.2013.08.013](https://doi.org/10.1016/j.geoderma.2013.08.013)
- Meinshausen N. 2006. Quantile regression forests. *J Mach Learn Res.* 7:983–999.
- Mondal B, Sekhon B, Sharma S, Singh M, Sahoo R, Barman A, Sinha Y, Chattopadhyay A, Banerjee K. 2017. VIS-NIR reflectance spectroscopy for assessment of soil microbiological properties. *Int J Curr Microbiol Appl Sci.* 6:719–728. doi:[10.20546/ijcmas.2017.612.075](https://doi.org/10.20546/ijcmas.2017.612.075).
- Mouazen AM, De Baerdemaeker J, Ramon H. 2005. Towards development of on-line soil moisture content sensor using a fibre-type NIR spectrophotometer. *Soil Tillage Res.* 80(1–2):171–183. doi:[10.1016/j.still.2004.03.022](https://doi.org/10.1016/j.still.2004.03.022).
- Mouazen AM, Maleki MR, De Baerdemaeker J, Ramon H. 2007. On-line measurement of some selected soil properties using a VIS-NIR sensor. *Soil Tillage Res.* 93(1):13–27. doi:[10.1016/j.still.2006.03.009](https://doi.org/10.1016/j.still.2006.03.009).
- Naimi S, Ayoubia S, Di Raimo LADL, Dematte JAM. 2022. Quantification of some intrinsic soil properties using proximal sensing in arid lands: application of Vis-NIR, MIR, and pXRF spectroscopy. *Geoderma Reg.* 28:e00484. doi:[10.1016/j.geodrs.2022.e00484](https://doi.org/10.1016/j.geodrs.2022.e00484).
- Ng W, Minasny B, Malone BP, Sarathjith MC, Das BS. 2019. Optimizing wavelength selection by using informative vectors for parsimonious infrared spectra modelling. *Comput Electron Agric.* 158:201–210. doi:[10.1016/j.compag.2019.02.003](https://doi.org/10.1016/j.compag.2019.02.003).

- Pal DK **2021**. Genesis and Usefulness of 0.7 nm Minerals (Kaolinite and Kaolin) in Indian Tropical Soils: Exploring Realm. *Clay Res.* 40(1):52–69. doi:[10.5958/0974-4509.2021.00006.1](https://doi.org/10.5958/0974-4509.2021.00006.1).
- Pinheiro ÉFM, Ceddia MB, Clingensmith CM, Grunwald S, Vasques GM. **2017**. Prediction of soil physical and chemical properties by visible and near-infrared diffuse reflectance spectroscopy in the central Amazon. *Remote Sens.* 9(4):293. doi:[10.3390/rs9040293](https://doi.org/10.3390/rs9040293).
- Piper CS. **1966**. Soil and plant analysis. Bombay; India: Hans Publishers.
- Pirie A, Singh B, Islam K. **2005**. Ultra-violet, visible, near-infrared, and mid-infrared diffuse reflectance spectroscopic techniques to predict several soil properties. *Soil Res.* 43(6):713–721. doi:[10.1071/SR04182](https://doi.org/10.1071/SR04182).
- Post JL, Noble PN. **1993**. The near-infrared combination band frequencies of dioctahedral smectites, micas, and illites. *Clays Clay Miner.* 41(6):639–644. doi:[10.1346/CCMN.1993.0410601](https://doi.org/10.1346/CCMN.1993.0410601).
- Reeves IIIJB, Follett RF, McCarty GW, Kimble JM. **2006**. Can near or mid-infrared diffuse reflectance spectroscopy be used to determine soil carbon pools? *Commun Soil Sci Plant Anal.* 37(15–20):2307–2325. doi:[10.1080/00103620600819461](https://doi.org/10.1080/00103620600819461).
- Richard LA. **1954**. Diagnosis and improvement of saline and alkalis soils. Washington DC: Agric. Handbook 60, US Dept. Agric; p. 160.
- Richter N, Jarmer T, Chabriat S, Oyonarte C, Hostert P, Kaufmann H. **2009**. Free iron oxide determination in Mediterranean soils using diffuse reflectance spectroscopy. *Soil Sci Soc Am J.* 73(1):72–81. doi:[10.2136/sssaj2008.0025](https://doi.org/10.2136/sssaj2008.0025).
- Rodionov A, Welp G, Damerow L, Berg T, Amelung W, Pätzold S. **2015**. Towards on-the-go field assessment of soil organic carbon using Vis–NIR diffuse reflectance spectroscopy: developing and testing a novel tractor-driven measuring chamber. *Soil Tillage Res.* 145:93–102. doi:[10.1016/j.still.2014.08.007](https://doi.org/10.1016/j.still.2014.08.007)
- Rossel RAV, Behrens T. **2010**. Using data mining to model and interpret soil diffuse reflectance spectra. *Geoderma.* 158(1–2):46–54. doi:[10.1016/j.geoderma.2009.12.025](https://doi.org/10.1016/j.geoderma.2009.12.025).
- Rossel RAV, McGlynn RN, McBratney AB. **2006a**. Determining the composition of mineral-organic mixes using UV–vis–NIR diffuse reflectance spectroscopy. *Geoderma.* 137(1–2):70–82. doi:[10.1016/j.geoderma.2006.07.004](https://doi.org/10.1016/j.geoderma.2006.07.004).
- Rossel RAV, Walvoort DJJ, McBratney AB, Janik LJ, Skjemstad JO. **2006b**. Visible, near-infrared, mid infrared or combined diffuse reflectance spectroscopy for simultaneous assessment of various soil properties. *Geoderma.* 131(1–2):59–75. doi:[10.1016/j.geoderma.2005.03.007](https://doi.org/10.1016/j.geoderma.2005.03.007).
- Santra P, Sahoo RN, Das BS, Samal RN, Pattanaik AK, Gupta VK. **2009**. Estimation of soil hydraulic properties using proximal spectral reflectance in visible, near-infrared, and shortwave-infrared (VIS-NIR-SWIR) region. *Geoderma.* 152(3–4):338–349. doi:[10.1016/j.geoderma.2009.07.001](https://doi.org/10.1016/j.geoderma.2009.07.001).
- Sarathjith MC, Das BS, Vasava HB, Mohanty B, Sahadevan AS, Wani SP, Sahrawat KL. **2014**. Diffuse reflectance spectroscopic approach for the characterization of soil aggregate size distribution. *Soil Sci Soc Am J.* 78(2):369–376. doi:[10.2136/sssaj2013.08.0377](https://doi.org/10.2136/sssaj2013.08.0377).
- Saxena RK, Verma KS, Srivastava R, Yadav J, Patel NK, Nasre RA, Barthwal AK, Shiwalkar AA, Londhe SL. **2003**. Spectral reflectance properties of some dominant soils occurring on different altitudinal zones in Uttaranchal Himalayas. *Agropedology.* 13(2):35–43.
- Schollenberger CJ, Simon RH. **1945**. Determination of exchange capacity and exchangeable bases in soil—ammonium acetate method. *Soil Sci.* 59(1):13–24. doi:[10.1097/00010694-194501000-00004](https://doi.org/10.1097/00010694-194501000-00004).
- Shivaprasad CR, Reddy RS, Sehgal J, Velayutham M. **1998**. Soils of Karnataka for optimizing land use. The report published by the National bureau of soil survey and land use planning. Nagpur; India: NBSS Publ. 47b (Soils of India Series); p. 1–111.
- Singh M, Srivastava R, Sethi M, Sood A. **2014**. Development of spectral reflectance methods and low-cost sensors for real-time application of variable rate inputs in precision farming. Ludhiana; India: National Agricultural Innovation Project (ICAR); Punjab Agricultural University.
- Soil Survey Staff. **2010**. Keys to Soil Taxonomy. 11th. Washington DC: USDA-NRCS.
- Solanke PC, Srivastava R, Prasad J, Nagaraju MSS, Patil NG, Nasre RA, Naitam RK, Wakode RR. **2021**. Spectral reflectance properties of vertisols and associated soils of Nagpur District in Maharashtra. *Journal of the Indian Society of Soil Science.* 69(1):21–27. doi:[10.5958/0974-0228.2021.00016.5](https://doi.org/10.5958/0974-0228.2021.00016.5).
- Srivastava R, Prasad J, Saxena R. **2004**. Spectral reflectance properties of some shrink-swell soils of Central India as influenced by soil properties. *Agropedology.* 14:45–54.
- Srivastava R, Sethi M, Yadav RK, Bundela DS, Singh M, Chattaraj S, Singh SK, Nasre RA, Bishnoi SR, Dhale S. **2017**. Visible–near infrared reflectance spectroscopy for rapid characterization of salt-affected soil in the Indo-Gangetic Plains of Haryana, India. *J Indian Soc Remote Sens.* 45(2):307–315. doi:[10.1007/s12524-016-0587-0](https://doi.org/10.1007/s12524-016-0587-0).
- Stenberg B. **2010**. Effects of soil sample pretreatments and standardised rewetting as interacted with sand classes on Vis–NIR predictions of clay and soil organic carbon. *Geoderma.* 158(1–2):15–22. doi:[10.1016/j.geoderma.2010.04.008](https://doi.org/10.1016/j.geoderma.2010.04.008).
- Stenberg B, Rosse RAV, Mouazen AM, Wetterlind J. **2010**. Visible and near-infrared spectroscopy in soil science. *Adv Agron.* 107:163–215. doi:[10.1016/S0065-2113\(10\)07005-7](https://doi.org/10.1016/S0065-2113(10)07005-7).
- Stevens A, Nocita M, Tóth G, Montanarella L, van Wesemael B. **2013**. Prediction of soil organic carbon at the European scale by visible and near infrared reflectance spectroscopy. *Plos One.* 8(6):e66409. doi:[10.1371/journal.pone.0066409](https://doi.org/10.1371/journal.pone.0066409).

- Stevens A, van Wesemael B, Bartholomeus H, Rosillon D, Tychon B, Ben-Dor E. **2008**. Laboratory, field and airborne spectroscopy for monitoring organic carbon content in agricultural soils. *Geoderma*. 144(1–2):395–404. doi:[10.1016/j.geoderma.2007.12.009](https://doi.org/10.1016/j.geoderma.2007.12.009).
- Tennesen BM. **2014**. Rare earth. *Science*. 346(6210):692–695. doi:[10.1126/science.346.6210.692](https://doi.org/10.1126/science.346.6210.692).
- Terra FS, Dematté JAM, Viscarra Rossel RA. **2015**. Spectral libraries for quantitative analyses of tropical Brazilian soils: comparing vis–NIR and mid-IR reflectance data. *Geoderma*. 255–256:81–93. doi:[10.1016/j.geoderma.2015.04.017](https://doi.org/10.1016/j.geoderma.2015.04.017)
- Udelhoven T, Emmerling C, Jarmer T. **2003**. Quantitative analysis of soil chemical properties with diffuse reflectance spectrometry and partial least-square regression: a feasibility study. *Plant Soil*. 251(2):319–329. doi:[10.1023/A:1023008322682](https://doi.org/10.1023/A:1023008322682).
- Vasques GM, Grunwald S, Sickman JO. **2009**. Modeling of soil organic carbon fractions using visible–near-infrared spectroscopy. *Soil Sci Soc Am J*. 73(1):176–184. doi:[10.2136/sssaj2008.0015](https://doi.org/10.2136/sssaj2008.0015).
- Vibhute AD, Kale KV, Mehrotra SC, Dhumal RK, Nagne AD. **2018**. Determination of soil physicochemical attributes in farming sites through visible, near-infrared diffuse reflectance spectroscopy and PLSR modeling. *Ecol Process*. 7 (1):1–12. doi:[10.1007/s11629-019-5789-9](https://doi.org/10.1007/s11629-019-5789-9).
- Walkley A, Black IA. **1934**. An examination of the Degtjareff method for determining soil organic matter and a proposed modification of the chromic acid titration method. *Soil Sci*. 37(1):29–38. doi:[10.1097/00010694-193401000-00003](https://doi.org/10.1097/00010694-193401000-00003).
- Zeraatpisheh M, Ayoubi S, Jafari A, Finke P. **2017**. Comparing the efficiency of digital and conventional soil mapping to predict soil types in a semi-arid region in Iran. *Geomorphology*. 285:186–204. doi:[10.1016/j.geomorph.2017.02.015](https://doi.org/10.1016/j.geomorph.2017.02.015)